Published in final edited form as:
J Immunol. 2008 September 1; 181(5): 3336–3345.

A PTB-dependent Program of mRNA Stability Initiates with CpG-mediated Activation of Primary B cells[1]

Joseph F. Porter[#], **Stefano Vavassori**[#], and **Lori R. Covey**[*]
Department of Cell Biology and Neuroscience, Rutgers University, Piscataway, NJ 08854

Abstract

The mRNA encoding CD154, a critical protein involved in both humoral and cell-mediated immune responses, is regulated at the post-transcriptional level by the binding of Complex I, a polypyrimidine tract-binding protein (PTB) containing complex, which acts to increase message stability at late times of activation. Our current work focuses on analyzing a similar complex in B cells, designated B-cpx I that is increased in B cells activated by CpG engagement of the TLR9 receptor but not by activation through CD40. Expression profiling of transcripts from primary B cells identified 31 mRNA transcripts with elevated PTB binding upon activation. Two of these transcripts, Rab8A and cyclin D2, contained binding sites for B-cpx I in their 3′ untranslated regions (3′ UTRs). Analysis of turnover of endogenous Rab8A transcript in B cells revealed that like CD154, the mRNA half-life ($t_{1/2}$) increased following activation and insertion of the Rab8A B-cpx I binding site into a heterologous transcript led to a 3-fold increase in stability. Also, shRNA down-regulation of PTB resulted in a corresponding decrease in Rab8A mRNA half-life. Overall these data strongly support a novel pathway of mRNA turnover that is expressed both in T cells and B cells and depends on the formation of a PTB-containing stability complex in response to cellular activation.

Keywords

3′UTR; TLR9; B cells; mRNA decay; Rab8A

Introduction

T-cell dependent (TD) B cell activation requires both cognate and non-cognate $CD4^+$ T cell interactions to induce a comprehensive humoral immune response against a wide range of pathogens. CD40 ligand (CD154 or CD40L) is critical for orchestrating this process (1,2) by binding to CD40 on antigen-activated B cells (3,4). Interaction between CD154 expressed on $CD4^+$ T cells and CD40 on B cells results in proliferation, differentiation, isotype switching, affinity maturation and the development of the memory cell compartment (3,5).

In contrast to TD B cell activation, T-cell independent (TI) mechanisms are not dependent on direct T cell interactions and are generally mediated by pathogenic surface antigens that express repetitive epitopes capable of crosslinking the B cell receptor (BCR) (6). Additionally, B cells express Toll-like receptors (TLR) that recognize conserved pathogen associated molecular

[1]This work was supported by grants from The National Institutes of Health (PO1 AI-57596) and The American Heart Association to L. R. C. and a post-doctoral fellowship from the New Jersey Commission on Cancer Research to J. F. P.

*Corresponding Author. Mailing address: B314 Nelson Hall, 604 Allison Road, Piscataway, New Jersey 08854. Phone: 732-445-4777. FAX: (732)-445-5870. E-mail: covey@biology.rutgers.edu.
[#]J. F. P and S. V. contributed equally to this work

Disclosures: The authors declare no conflict of interest with the results presented.

patterns (PAMPs) such as LPS, peptidoglycan, dsRNA, flagelin, and unmethylated CpG repetitive DNA (6-8). The TLR9 protein has been shown to bind specifically to unmethylated-CpG DNA and is expressed on endosomal membranes of both primary and transformed B cells (9). TLR9 engagement induces proliferation, IgG class switch recombination and the expression of cytokines IL-6 and IL-12 (10-12) whereas dual signaling through CD40 and TLR9 provides synergistic activation of tonsillar B cells into antibody producing cells (13).

Activation-induced genes are often regulated via differential transcriptional processes (reviewed in (14,15)), although post-transcriptional control represents a second major pathway of regulation (reviewed in (16,17)). Differential RNA decay acts to quickly integrate distinct cellular signals to change the expression of a particular gene or set of genes necessary for an appropriate immune response. A major pathway of RNA turnover involves the interaction of several RNA binding proteins with AU-rich elements or AREs, located in the 3′ untranslated regions (UTR) of cytokine and growth factor mRNAs (reviewed in (17,18)). These RNA binding proteins include those such as AUF1 and tristetraprolin (TTP) that act to destabilize the associated transcript and HuR that has been shown to stabilize the targeted message. mRNA decay initiates with the degradation of the poly-A tail and the remaining transcript is recognized and degraded either by a 5′ or 3′ exonuclease pathway (reviewed in (17)). In contrast, non-ARE pathways often involve a stabilizing protein that binds to a specific sequence in an mRNA and the absence of binding leads to increased turnover of the message. For example, one important class of stability elements is distinguished by a high (CU) content and the ability to extend the half-life ($t_{1/2}$) of long-lived messages (reviewed in (19)). The most widely studied element in this class is the erythroid-specific mRNA stability determinant, composed of a C-rich sequence in a highly pyrimidine-rich region of the α-globin 3′UTR. This element is functionally linked to the stability of the α-globin transcript and binds a set of proteins, termed the α-complex, which contains α-CP-1 and α-CP-2 as well as additional cofactors (20,21).

Over the past several years our lab has demonstrated the importance of a non-ARE pathway of post-transcriptional control in the regulation of CD154 expression in differentially activated primary $CD4^+$ T cells. At early times of anti-CD3 activation the CD154 message is highly unstable with a $t_{1/2}$ of less than 40 min however at later times of activation the $t_{1/2}$ is increased to greater than 2 h (22). A sequence was identified in the CD154 3′UTR that contained three adjacent CU-rich binding sites that bound either a dominant RNA binding complex termed Complex I, or a minor complex, termed Complex II (23). Subsequent work revealed that the major protein in Complex I was polypyrimidine tract-binding protein (PTB or hnRNP I) (24) and nucleolin was a second component that bound both to PTB and the CD154 transcript (25). Importantly we demonstrated that Complex I played a critical role in stabilizing the CD154 transcript at late times of activation (24).

In this report we extend our previous work on the role of Complex I-mediated mRNA stability in activated T cells by identifying a PTB-containing complex (B-cpx I) that is regulated in response to B cell activation. Specifically we show that B-cpx I is expressed in response to engagement of TLR9 and only minimally to CD40 signals. Microarray analysis identified a subset of transcripts that interacted with PTB in activated B cells and further work identified a transcript, Rab8A, which was stabilized in a PTB-dependent process in response to CpG activation. Together our findings reveal that a PTB-regulated pathway of mRNA decay common to both activated T cells and B cells. Furthermore, in B cells, this pathway appears to be highly dependent on a specific activation pathway since PTB-regulated decay is most prominently observed with TLR9 but not CD40 signals.

Materials and Methods

Antibodies, Cell Lines and CpG Oligodeoxynucleotides (ODN)

The anti-PTB hybridoma CRL-2501 was obtained from American Type Culture Collection (ATCC) (Manassas, VA). Anti-PTB mAb was purified from conditioned media using Protein A beads. The Jurkat/D1.1 cell line was obtained from Dr. S. Lederman (Columbia U.) and cultured as previously described (25). The D11-LCL^{tet} line was generated using a mini-EBV vector expressing the LMP1 gene under the control of a tetracycline responsive promoter (26) and from PBMCs obtained from a healthy volunteer. Generation and maintenance of this line has recently been described (27). The 10103 CpG ODN was obtained from Coley Pharmaceutical Canada (Ottawa, Ontario).

Primary B Cell Isolation and Activation

Heparinized blood from healthy volunteers was obtained as fractionated buffy coats from the New York Blood Center (NY, NY) and PBMCs were purified by centrifugation over Ficol as previously described (24). Primary B cells were isolated using Dynabeads CD19 Pan B magnetic beads according to the manufacture's instructions (Invitrogen Corp., Carlsbad, CA). For a subset of experiments, CD19 selected cells were incubated for 30 min on a 10-cm petri dish coated with 5ml of 25μg/ml anti-IgG (Southern Biotech, Birmingham, AL) to remove IgG$^+$ B cells. The unattached cells (CD19$^+$/IgG$^-$) were removed by pipetting and isolated primary B cells were cultured in RPMI 1640 supplemented with 10% FCS, 2mM glutamine and 1mM sodium pyruvate at a concentration of 2.5×10^6 cells/ml. B cells were activated for 48 h with the following stimulators alone or in combination: 3μM 10103 CpG ODN, membranes purified from the 293 cell line expressing CD40L (293CD40L) as previously described (27) and 200U/ml IL-4 (Peprotech, Inc., Rocky Hill, NJ).

Cytoplasmic Protein Extracts

Primary CD19$^+$/IgG$^-$ or D11-LMP^{tet} B cells were washed in PBS and resuspended in extraction buffer (0.2% Nonidet P-40, 40mM KCl, 10mM HEPES (pH 7.9), 3mM $MgCl_2$, 5% glycerol, 1mM DTT and 1× protease inhibitor cocktail (Sigma Chemical Co., St. Louis, MO)) as described previously (28). Cells were incubated on ice for 5 min, centrifuged at 12000 × g for 10 min and the supernatant collected.

RNA Immunoprecipitation

For RNA immunoprecipitation, protein A beads (Santa Cruz Biotechnology, Santa Cruz, CA) were coated with anti-PTB mAb (ATCC) for the microarray and either anti-PTB mAb or $IgG2_b$ (Southern Biotech) for the RT-PCR used for binding verification. Cells were washed 2× in PBS and cytoplasmic extracts were prepared as described above. Cellular equivalents of DNase I-treated cytoplasmic extract (~100-200μg from resting or CpG-activated-primary B cells) were loaded onto the antibody-coated beads resuspended in NT2 buffer (50mM Tris (pH 7.4), 150mM NaCl, 1mM $MgCl_2$, 0.05% Nonidet P-40, 20mM EDTA, 1mM DTT, 200U/ml rRNasin (Promega, Madison, WI)). The bead/extract mixture was incubated on a rotator at 4° C for 4 h, washed 6× with ice-cold NT2 buffer, resuspended in NT2 buffer + 0.1% SDS and 30μg proteinase K followed by incubation at 55°C for 2-3 h. The supernatant was collected and RNA isolated by phenol-chloroform extraction and ethanol precipitation.

Microarray Experiments

RNA quantity and quality were assessed by NanoDrop spectrophotometer and electrophoresis using the Agilent Bioanalyzer 2100 (Quantum Analytics, Inc., Foster City, CA) prior to cDNA synthesis. Immunoprecipitated RNA (1μg) was used to synthesize cDNA using Superscript II and oligo(dT_{15}) following the manufacturer's protocol (Invitrogen). Biotin-labeled cRNA was

generated using the ENZO BioArray RNA transcript labeling kit and fragmented at 94°C for 35 min. All samples (15μg) were subjected to gene expression analysis via the Affymetrix Human U133A 2.0 high-density oligonucleotide array, which queried 18,400 human transcripts (Affymetrix, Inc., Santa Clara, CA). Processing, detection and quantification was performed according to the manufacturer's directions. Array analysis was carried out with two independently isolated and immunoprecipitated RNA samples at the Transcriptional Profiling Shared Resource of the Cancer Institute of New Jersey (New Brunswick, NJ). The third microarray was performed in a similar fashion using the Affymetrix Human U133 Plus 2.0 high-density oligonucleotide array which queried 47,400 human transcripts including the 18,400 on the U133A array (Affymetrix, Inc., Santa Clara, CA) according to the manufacturer's protocol at the Bionomics Research and Technology Center at EOHSI, Rutgers University (Piscataway, NJ).

Each set of arrays was normalized to each other and a comparison analysis was performed for each set of arrays using Affymetrix MAS 5.0. to determine which transcripts were significantly increased (2-fold or more). Wilcoxon's signed rank test was used to generate change p-values to indicate the likelihood of change in transcript expression level.

RT-PCR to Analyze Transcript Enrichment by anti-PTB mAb

RNAs were immunoprecipitated as described above with IgG_{2b} or anti-PTB mAb from cytoplasmic extracts of CpG-activated $CD19^+$ B cells. Reverse transcription reactions were carried out using Transcriptor First Strand cDNA Synthesis Kit (Roche). 1/10th vol equivalent of cytoplasmic extracts was also reverse transcribed and used as a positive control for each reaction. PCR reactions (25μl) were performed with 0.3μM of 3′ and 5′ primers and FastStart Taq DNA polymerase (Roche). The cycling parameters were as follows: 94°C for 5 min; 40 cycles of 94°C for 10 sec; 10 sec at 60°C; and 72°C for 20 sec. Sets of intron-spanning primers were designed using the Universal Probe Library Assay Design Center (http://www.roche-applied-science.com/sis/rtpcr/upl/adc.jsp) with the exception of primers used for β–actin transcript detection (see primers used in qPCR reaction).

RNA probes

The Complex I Xba I-Hae III probe was synthesized as previously described (24). Primers used for PCR amplification of gene-specific RNA probes and mapping of the Rab8A binding site are as follows: cyclin D2 Fwd 5′CGTAATACGACTCACTATAG GGAAGGAATCCTGGATTTTG 3′, Rev 5′ TAGGATTTGGCCAAAAGAGGGGAAGGATCA 3′; CD20 Fwd 5′ CGTAATACGACTCACTATAGGGGTGATTTCTTCTGTTTTC 3′, Rev 5′ AAGCTATGCTGTTTTTACAAAAAACAGATG 3′; SET Fwd CGTAATACGACTCACTATAGGGATAGAACACTGATGGATT, Rev 5′ CAGAGCGAAGGGAGCAGGTTTTTCTTTTTT 3′; RAB8 Fwd 5′ CGTAATACGACTCACTATAGGGCCTTTTCTTTTTTTCTTT 3′, Rev 5′ AAAAGAAACGATGATGCCAATGGTTTGGAT 3′; RAB8 M5′-9 Fwd 5′ CGTAATACGACTCACTATAGGGTTTTTCTTTCTTTTTTTT 3′; RAB8 M5′-21 Fwd 5′ CGTAATACGACTCACTATAGGGTTTTTTTTTTTCCTCCTT 3′; RAB8 M3′-8 Rev 5′ CGATGATGCCAATGGTTTGGATTGACAGCA 3′; RAB8 M3′-29 Rev 5′ TTGACAGCAGCTTAAGGAGGAAAA 3′; RAB8 M3′-34 Rev 5′ AGCAGCTTAAGGAGGAAAAAAAAA 3′. RNA probes were synthesized and labeled with [α-^{32}P]rUTP (Perkin Elmer Life Sciences, Boston, MA) using 100ng of purified PCR product and T7 polymerase (Promega). The RNA probe was purified by elution through a G25 column (Amersham Biosciences, Piscataway, NJ).

RNA Electromobility Shift Assay (R-EMSA)

Reactions were prepared in RNA binding buffer with 4ng E. *coli* tRNA, 5μg cytoplasmic extract and 40,000 cpm of RNA probe for primary B cells or 5000cpm for D11-LCL^{tet} cells. The reactions were incubated for 20 min at room temperature to allow for complex formation followed by the addition of 1μl RNase mix containing 40U RNase T_1 10ng RNaseA, 0.01U RNase V_1 (Ambion, Austin, TX) for primary B cells and a 1:8 dilution of this RNase mix for D11-LCL^{tet} cells. Samples were incubated at 37°C for 30 min, 2 μl of 50μg/ml heparin was added and reactions were incubated on ice for 10 min. Protein-RNA complexes were separated on a 7% native acrylamide gel in 0.25× TBE. Supershift experiments were performed with 1μg of anti-PTB or control $IgG2_b$ antibodies added to the reactions for 1 h at RT prior to addition of the probe.

Luciferase Constructs and Assays

The 52bp minimum binding site for B-cpx I identified in the 3′UTR of Rab8A was amplified using PfuUltra Fusion HS DNA polymerase (Stratagene, La Jolla, CA) and D1 1-LCL^{tet} cDNA using the following primers: Rabd52 3′Fwd,5′-GGGTGTCACCAGTCCAAACCATTGGCATCA-3′ and Rabd52 3′Rev, 5′-TGATGCCAATGGTTTGGACTGGTGACACCC 3′. The amplified region was cloned into the *XbaI* site located in the 3′UTR of the *Renilla* luciferase gene of the pRLSV40 plasmid (Promega). A control vector was constructed that contained the 52bp sequence ligated into the *XbaI* site in the reverse orientation. The pGL23a plasmid containing the firefly luciferase under the control of the CD23a promoter (Dr. S. Lederman, Columbia, University) was used as a transfection control in all luciferase assays performed.

Approximately, 5×10^6 D11-LCL^{tet} cells were grown in 1μg/ml tetracycline and incubated with 2.5μg of the binding site construct and 25μg of pGL23a control plasmid. The cells were transfected with 1 pulse of 250mV and 960μF capacitance using an electroporator (Biorad Corp., Hercules, CA), resuspended in media plus tetracycline and 3μM CpG ODN and incubated for 48 h. After incubation, cells were harvested and extracts prepared for analysis of luciferase activity using a Dual Luciferase Assay Kit (Promega) and a Glomax Luminometer (Promega). Results were normalized to *firefly* luciferase activity to account for differences in transfection efficiency.

5,6-Dichlorobenzimidizole 1-β-D-ribofuranoside (DRB) Treatment and RNA Isolation

To analyze the decay rate of Rab8A in primary B cells, 2×10^7 $CD19^+/IgG^-$ B cells were incubated with 3uM CpG ODN for 48 h followed by 50μg/ml DRB. A total of 5×10^6 cells were removed at each time point over a 4 h time course. RNA was isolated using the High Pure RNA Isolation Kit (Roche Diagnostics, Indianapolis, IN).

The effect of the Rab8A B-cpx I binding region on mRNA stability was determined by transiently transfecting 3×10^7 D11-LCL^{tet} cells with the different Rab8A luciferase constructs using the Amaxa Biosystems Transfection System (Cologne, Germany) followed by incubation with 3μM CpG for 24 h. Treatment with DRB over a time course was carried out as described above. RNA was prepared using Trizol (Invitrogen) followed by treatment with Turbo DNase (Ambion).

cDNA Synthesis and Quantitative-Real Time PCR (QPCR)

cDNA was synthesized from DRB-treated RNA samples using the Transcriptor First Strand cDNA Synthesis Kit (Roche). qPCR was performed on the cDNA using the following primers: 5′GCATCCTCACCCTGAAGTA-3′ together with 5′-TGTGGTGCCAGATTTTGTCC-3′ to detect the β-actin transcript and 5′-CCAAGACACAAGGCATTCCA-3′ and 5′-

GTCCCAGTCGCAGTCCCTAT-3′ to detect the Rab8A transcript. Amplification reactions were carried out using both the Mx4000 Multiplex PCR System and FastStart SYBR Green Master Mix (Rox) according to the manufacturer's directions (Stratagene and Roche, respectively). After the amplification a melt curve was performed to ensure amplicon homogeneity. Decay of a specific RNA transcript was determined by the $2^{-\Delta\Delta Ct}$ method comparing each time point to the zero time point to quantify the percent RNA remaining (29, 30) using the MxPro-Mx3000P software supplied with the Mx4000 Multiplex PCR system.

Statistical Analysis

For comparison of two samples a two-tailed Student's T-test was used. Significance was set at $P< 0.05$. Data in figures is shown as mean +/- SEM unless otherwise indicated.

shRNA knock-down of PTB

To generate the pLVTHM-U6-shPTB and pLVTHM-U6-shCTRL vectors the following primers were annealed and cloned into the *Hind*III and *Eco*RI sites of the pSilencer2.1-U6 hygro (Ambion, Austin TX) Primers 5′-GATCCAACTTCCATCATTCCAGAGAACTTGCTTCTTCTCTGGAATGATGGAAGTTTTT TTTGGAAA-3′ and 5′ AGCTTTTCCAAAAAAAACTTCCATCATTCCAGAGAAGAAGCAAGTTCTCTGGAATG ATGGAAGTTG-3′ (U6-shPTB) and 5′ GATCCAATCAGACGTGGACCAGAAGAGAGATCTTCTGGTCCACGTCTGATTTTTTT TGGAAA-3′ and 5′-AGCTTTTCCAAAAAAAATCAGACGTGGACCAGAAGATCTCTCTTCTGGTCCACGTCT GATTG-3′ (U6-shControl). The sequence containing the U6 promoter and shRNA was then PCR amplified from these vectors using the following primer set: 5′-CCATCGATGGAGCTTTTCCAAAAAAAACTT-3′ and 5′-CAGAAAGGTGACCCCTTAAGCTTCTAGAAG-3′. These PCR products were then cut with the restriction enzymes *Cla*I and *Bgl*II and cloned into the corresponding sites of the pLVTHM vector (Addgene plasmid 12247).

Viral particles were packaged by transfection of 293T cells with either pLVTHM-U6-shPTB or pLVTHM-U6-shControl together with the virus packaging plasmids pSPAX2 (Addgene plasmid 12260) and pCI-VSVG (Addgene plasmid 1733), both obtained from D. Trono (Ecole Polytechnique Fédérale de Lausanne, Lausanne, Switzerland), using FuGENE HD Transfection Reagent (Roche). Culture supernatants were collected every 12h. 5×10^7 D11-LCL^{tet} cells were infected with 5ml of viral supernatant in a final volume of 20ml. 48 h post-infection an aliquot of 1×10^7 cells was incubated in media containing 10mg/ml doxycycline for 24 h. These cells were then analyzed for GFP expression by FACS analysis to determine the percentage of infected cells. Cytoplasmic extracts were also analyzed by western blot to determine the level of PTB between cells expressing control shCTRL or shPTB. The remaining cells were incubated with 50μg/ml DRB over a 3 h time course and RNA isolated and analyzed by qPCR as described above.

Results

A PTB-containing complex (*B-cpx I*) is upregulated in activated B cells

Primary CD19$^+$ B cells were isolated from human peripheral blood and activated with CD154-expressing 293 cells or CpG. RNA electromobility shift assays (R-EMSA) were carried out with cytoplasmic extracts from CpG, CD154, CpG + CD154 and CD154 + IL-4 stimulated cells and an *in vitro* synthesized and labeled RNA probe containing the CD154 stability element (termed Xba I-Hae III) (Fig. 1A). This probe binds Complex I in extracts from both late activated CD4$^+$ T cells and Jurkat/D1.1 T cells (24). As shown in Fig. 1B, strong complex

binding was observed with extracts from B cells stimulated with CpG (lanes 5, 6, and 8) although there was a low level of complex formed with extracts from cells stimulated both with CD154 and CD154 + IL-4 (lanes 4 and 7). Little to no complex binding activity was seen with extracts from resting B cells (lane 3). Since we had previously shown that PTB is a major protein in Complex I from activated T cells, R-EMSA was carried out using anti-PTB antibodies to determine whether PTB is present in the B cell complex. Accordingly, PTB was also found to be a major component of the complex in activated B cells (lane 9) and this result was confirmed by UV-cross linking (data not shown). Based on the similarity of this complex to Complex I, we designated it, B cell-Complex I or B-cpx I.

A select subset of transcripts binds PTB in CpG-activated B cells

To identify transcripts bound by B-cpx I, cytoplasmic extracts from CpG-treated and resting $CD19^+$ B cells were immunoprecipitated with anti-PTB antibodies and bound transcripts isolated, reversed transcribed and used as probes on the U133A 2.0 human oligonucleotide array. Results revealed that 48 transcripts gave positive signals on 2 independent arrays with an approximate 2-fold or greater increase over resting B cells on each array. To eliminate any contribution from the small percentage (<10 %) of IgG^+ B cells isolated in the $CD19^+$ pool another set of RNAs was immunoprecipitated from cytoplasmic extracts of CpG-treated and resting $CD19^+/IgG^-$ B cells. These RNAs were analyzed on the U133 Plus 2.0 high-density oligonucleotide array and 31 transcripts were shown to be increased by 2-fold or greater on all 3 arrays (Table I).

Confirmation of the compiled microarray results was carried out by immunoprecipitating cytoplasmic extracts from CpG-activated $CD19^+$ B cells with either anti-PTB or control ($IgG2_b$) antibodies followed by assessing the subset of identified mRNAs for specific binding. To show primer specificity the same reactions were performed using non-immunoprecipitated cytoplasmic extracts with 10 fold-less starting material (Lane 1). PCR reactions were continued to saturation. As shown in Table II, all transcripts tested (25 of 31 total) gave positive signals in the PTB-selected fraction compared to the Ig control fraction. To show that the positively selected transcripts represented a true sub-population, PCR amplification of the PTB-selected and control samples was carried out with primers to GAPDH and β-actin. Notably, there was no amplification of these transcripts in the selected or control populations confirming the specificity of the immunoprecipitation. These findings demonstrated that a subset of transcripts in B cells activated with CpG bound specifically to PTB and therefore were potential targets for B-cpx I binding.

B-cpx I binds to the Rab8A and cyclin D2 3′UTRs

Because of inherent limitations associated with obtaining appropriate cell numbers to carry out biochemical assays, we sought to identify a human B cell line that showed similar characteristics relative to B-cpx I binding of specific target RNAs. The D11-LCL^{tet} line is an IgM^+ B cell line that undergoes cell division in response to LMP1 expression in the presence of tetracycline (26,27). Using RNA binding assays we found that the D11-LCL^{tet} line constitutively expressed B-cpx I in the presence and absence of tetracycline however, there was an increase in complex binding when cells were activated with CpG (Fig. 2A). To determine whether B-cpx I bound specifically to motifs within the 3′UTR of array-identified transcripts, 3′UTRs were scanned for potential PTB binding motifs (UCUU) that were grouped together in the context of a pyrimidine-rich tract similar to the Complex I binding region in the CD154 transcript (23). Initial experiments were carried out with four transcripts, Rab8A, cyclin D2, CD20 and SET, which contained 5, 9, 9 and 4 potential 3′UTR PTB binding sites, respectively (data not shown). Extracts from D11-LCL^{tet} cells were stimulated with CpG for 48 hr and PTB-specific complexes identified by the addition of anti-PTB antibodies to a subset of *in vitro* binding reactions. Regions of each 3′UTR that span putative PTB binding sites were

used as *in vitro*-labeled probes. As shown in Fig. 2B, only RNA probes generated from Rab8A and cyclin D2 bound a potential B-cpx I-like complex (lanes 9-11 and 15-17, respectively). The lack of binding to the sub-regions of the CD20 and the SET 3′UTRs suggested that either PTB binding occurred at sites outside the targeted regions or that PTB-specific binding to these transcripts was unstable during the R-EMSA reaction.

Differential turnover of Rab8a mRNA in response to CpG-mediated B cell activation

To extend the analysis of B-cpx I to include functional properties similar to Complex I, we monitored the patterns of Rab8A and cyclin D2 RNA stability in resting versus 48 h CpG-activated $CD19^+$ B cells. Following activation, cells were incubated with DRB to arrest transcription for different times over a 4 h time course and RNA isolated from each time point. Similar to what was observed with CD154 in late-activated $CD4^+$ T cells, CpG activation of B cells was found to induce an increase in Rab8A RNA stability from a $t_{1/2}$ of ~1.3 h to ~2.6 h. In contrast, the cyclin D2 transcript showed no activation-induced stabilization over the same time course (Fig. 3). These findings suggested that only a subset of transcripts that bind PTB within their 3′UTRs are regulated in response to activation. One difference in the binding of PTB to the Rab8A and cyclin D2 transcripts was that the avidity of binding was much higher with the Rab8A transcript and this property may influence whether or not B-cpx I can stabilize a transcript or not (Fig. 2B). The fact that CpG increases Rab8A transcript stability extends the level of similarity between the regulation of the Rab8A and CD154 transcripts and strongly suggests that B-cpx I is involved in modulating the turnover of the Rab8A mRNA in an activation-dependent manner.

Identification of B-cpx I binding sites in the Rab8A 3′UTR

Analysis of the 258 nt sequence within the Rab8A 3′UTR that binds PTB revealed a CU-rich sequence of 81 nt that was highly pyrimidine rich and indicative of PTB binding sites (Fig. 4A). To identify minimum B-cpx I binding sites within this region, R-EMSA was carried out with a set of *in vitro* transcribed RNA probes that spanned the CU-rich region. As shown in Fig. 4B, the probes initiating with nt 1999, M (lane 13), M3′-8 (lane 16), M3′-29 (lane 17) and M3′-34 (lane 18) formed complex whereas probes M5′-9 and M5′-21, which began 9 nt and 21 nt downstream of 1999 and terminated with nt 2079 did not. This suggested that the 5′ boundary of the binding site was between nt 1999 and 2008. The 3′ boundary required for optimal binding was located downstream of nt 2050 (lanes 16-18) based on the decrease in complex formation with the M3′-34. Therefore, the minimal B-cpx I binding region in Rab8A mRNA was defined as a 52 nt region between nt 1999 and nt 2051.

The B-cpx I binding motif increases the expression of luciferase in vivo

To characterize the functional capacity of the B-cpx I binding site in the Rab8A transcript we established a luciferase-based expression system in which the 52bp B-cpx I minimum binding site from the Rab8A 3′UTR was introduced into the 3′ non-coding region of the *Renilla* luciferase operon in the pRLSV40 vector (termed, pRLRab52). A vector containing the 52bp insert in the reverse orientation was used as control (termed, pRLComp). The constructs were transiently transfected into $D11\text{-}LCL^{tet}$ cells, treated with CpG and analyzed for luciferase activity 48 h later. Insertion of the Rab8A 52bp minimum binding site increased luciferase activity approximately 4-fold over the control construct suggesting that the introduced element was having an effect either at the level of message stability or translation (Fig5A). Fig. 5B shows the results of three independent experiments that analyzed decay at 0, 1 and 4 h post-DRB addition and 48 h after transfection of the pRLRab52 and pRLComp plasmids. *Renilla* RNA containing the Rab52 insert was more stable than RNA containing the control insert lending strong support for a role of the Rab52 insert in mRNA turnover.

PTB stabilizes the Rab8A transcript in CpG-activated B cells

The effect of PTB on Rab8A transcript stabilization *in vivo* was assessed by infecting D11-LCL^{tet} cells with the retroviral vector (pLVTHM-U6) constitutively expressing either shRNA against PTB (shPTB) or a control sequence containing a scrambled shRNA (shCTRL). The pLVTHM-U6 vector also expresses eGFP under the control of a doxycycline-inducible promoter to allow the assessment of infection efficiency by FACS. Since the level of B-cpx I was increased when D11-LCL^{tet} cells were cultured in the presence of CpG (Fig. 2A) we wanted to assess the effect of Rab8A RNA stability in these cells grown either with tetracycline or 3 μM CpG. As shown in Fig. 6A, a significant majority of the cells were GFP positive 4 days following infection with the packaged pLVTHM-U6 vectors and infection corresponded to a distinct down regulation of the three isoforms of cytoplasmic PTB (PTB-1, PTB-2 and PTB-4) even after two days of CpG treatment (Fig. 6B). To establish whether this level of PTB downregulation affected Rab8A transcript stability, cells were infected with virus and grown continuously either with or without tetracycline for 4 days followed by activation of one culture with 3μM CpG for 48 h. Both cell populations were treated with DRB over a 3 h time course and RNA isolated at intervening time points. Overall CpG activation of the D11-LCL^{tet} cells led to an increase in the $t_{1/2}$ from approximately 95 min to greater than 3 hr (Fig. 6C and D, compare shCTRL curves). This increase was very similar to the increase in Rab8A stability that was observed in primary B cells (Fig. 3) and confirmed that the pathways leading to B-cpx I stability are present in the D11-LCL^{tet} cells. Importantly, introduction of the shPTB into either population decreased Rab8A RNA stability although the change was much greater in cells activated with CpG where the $t_{1/2}$ decreased from 3 h to approximately 90 min (Fig. 6D). This change closely mirrors the difference in Rab8A transcript stability in CpG versus tetracycline-exposed D11-LCL^{tet} cells and supports a model whereby transcript stability is a direct function of PTB binding. Thus, these findings strongly support a critical role for PTB in actively stabilizing the Rab8A transcript in CpG-activated B cells and both B cells and T cells clearly maintain an activation-induced RNA stability pathway that is dependent on PTB.

Discussion

Post-transcriptional regulation via RNA turnover is a critical factor that maintains appropriate levels of specific gene products during an ongoing immune response. While ARE-mediated decay has been extensively characterized and shown to be important for the expression of different inflammatory cytokines and growth factors, other pathways of regulated decay are much less well described. RNA-focused programs of gene expression have become increasingly important areas of study, particularly with respect to how these programs interface with more well characterized transcriptional and translational processes. Our past work defined both *cis*- and *trans*-acting factors required for an activation-dependent RNA decay program that regulates the expression of CD154 in activated CD4$^+$ T cells. The goal of this current study was to establish whether B cells also utilize a program of PTB- and activation-dependent mRNA turnover and if they do, to identify specific transcripts that are regulated by this mechanism.

The identification and characterization of the Rab8A mRNA as a B-cpx I-regulated transcript demonstrates that an activation-regulated process involving PTB is functioning in B cells. Rab proteins are members of the Ras GTPase superfamily and are known to function in both constitutive and regulated exocytosis, endocytosis and transcytosis (reviewed in (31)). Although the exact role for Rab in lymphocyte function is unknown, these functions are closely linked to lymphocyte activation and increased expression of Rab8A would likely be required during activation-induced proliferation, motility and antigen processing. Our current work adds Rab8A to a growing list of transcripts, which includes CD154 (24,32) insulin (33), vascular endothelial growth factor (34) and iNOS (35), that are regulated by PTB. Based on the fact

that one of the four transcripts tested (out of 31) showed PTB-dependent activation-induced turnover leads us to expect that a number of additional transcripts in B cells would also be regulated in an analogous manner. Additionally, since many more transcripts were identified on the larger array (Array #3) as showing enhanced PTB binding, we predict that the initial 31 transcripts identified is a conservative estimation of the number of transcripts regulated by PTB in response to activation. Although some of the transcripts identified on the arrays could merely reflect an overall increase in transcript binding that is unrelated to either B-cpx I or activation-induced decay, our expectation is that approximately 25% would demonstrate an activation-linked correspondence between B-cpx I and mRNA decay. Also, as we observed with cyclin D2, some transcripts may bind B-cpx I but do not show activation-induced stability. We hypothesize that the failure of cyclin D2 to be stabilized by B-cpx I may be related to the relatively low level of binding in CpG-activated cells (Fig. 2). This type of relationship has been demonstrated with tristetraprolin (TTP), an ARE-binding protein, and transcripts containing variations of the ARE motif. Specifically, a direct link was observed between binding affinity and mRNA decay using a number of distinct transcripts that varied in their affinity for TTP (36). In future work, we will explore the underlying differences in the Rab8A and cyclin D2 transcripts that lead to distinct modes of regulation upon activation.

PTB exits as three isoforms generated by differential splicing and the expression of each isoform can vary according to the tissue or cell type (37,38). PTB is monomeric in the reducing intracellular environment (39) and the binding sites defined for the RNA binding domains or RBDs are UCU (RBD1 and 4), UCNU (RBD2) and UCUCU (RBD3) (40). Sites identical if not similar to these are present in close proximity within the defined pyrimidine-rich minimum binding sites for both Complex I (CD154) and B-cpx I (Rab8A). In fact, the Rab8A site contains 3 UCU binding motifs in close proximity to each other. It is possible that monomeric PTB binds to these motifs, particularly the first motif given the fact that removal of the first UCU motif, as in the M5′-9 probe (Fig. 4), completely eliminates B-cpx I binding. Interestingly, the last 13 nt of the minimal binding region lack a pyrimidine-rich motif suggesting that binding of a second RNA binding protein may be required for efficient complex formation. This possibility is supported by other work demonstrating the association of PTB with such RNA binding proteins as nucleolin (25) and cold shock domain (CSD or Y-box) proteins (34). Alternatively, the 3′sequences may be involved in establishing a secondary structure important for PTB binding.

The RNA interference results clearly demonstrate that PTB confers significant stability on the Rab8A transcript in CpG-activated D11-LCL^{tet} cells and supports a model whereby induction by TLR9 signaling of B-cpx I activity directly regulates message stability. Since we observe PTB in the cytoplasm of both activated and non-activated B cells (data not shown), TLR9 signaling may induce a modification of PTB that allows it to form B-cpx I upon activation. This type of modification may be reminiscent of phosphorylation changes associated with the nucleocytoplasmic transport of PTB. Specifically, the 3,5-cAMP-dependent protein kinase (PKA) was shown to directly phosphorylate PTB on a conserved Ser-16 and this modification led to the accumulation of PTB in the cytoplasm (41).

The segregation of B-cpx I activity with CpG- and not CD40-activation was unexpected given that we had observed Complex I activity in differentially activated CD4$^+$ T cells (22). This absence of B-cpx-I activity was not due to a lack of CD40 responsiveness since signaling through either TLR9 or CD40 resulted in B cell proliferation and the expression of multiple activation markers (data not shown). The one marker that was positively associated with B-cpx I activity was upregulation of CD20. Enhanced expression of CD20 in human B cells has been shown to be controlled by ERK-dependent mechanisms (42) suggesting that B-cpx I may also be regulated by this pathway. This possibility is consistent with our findings relative to CD40 activation since CD40-mediated ERK/MAPK activity appears to require prior

stimulation through the BCR (43). In our experiments, B cells were activated through CD40 without BCR stimulation suggesting an absence of both ERK activation and B-cpx-I activity.

In conclusion, these findings expand our understanding of regulated mRNA decay in activated lymphocytes by demonstrating a common pathway of RNA turnover in both T cells and B cells. This pathway is dependent on the expression of a cytoplasmic PTB-containing complex that stabilizes mRNAs upon cellular activation. The unexpected finding that PTB-mediated stability was dependent on specific activation programs allows us to focus future work on identifying signaling pathways that directly engage the B-cpx I activity and deciphering mechanisms that relate mRNA stability to complex formation.

Acknowledgments

We acknowledge Lindsay Ordower for her expert technical assistance and thank the other members of the Covey lab for helpful discussions and critical comments on the manuscript. We are very grateful to Dr. Terri Goss Kinzy (Robert Wood Johnson Medical School) for valuable comments and criticism.

References

1. Armitage RJ, Fanslow WC, Strockbine L, Sato TA, Clifford KN, MacDuff BM, Anderson DM, Gimpel SD, Davis-Smith T, Maliszewski CR, Clark EA, Smith CA, Grabstein KH, Cosman D, Spriggs MK. Molecular and biological characterization of a murine ligand for CD40. Nature 1992;357:80–82. [PubMed: 1374165]
2. Hollenbaugh D, Grosmaire LS, Kullas CD, Chalupny NJ, Braesch-Andersen S, Noelle RJ, Stamenkovic I, Ledbetter JA, Aruffo A. The human T cell antigen gp39, a member of the TNF gene family, is a ligand for the CD40 receptor: expression of a soluble form of gp39 with B cell co-stimulatory activity. Embo J 1992;11:4313–4321. [PubMed: 1385114]
3. Bishop GA, Haxhinasto SA, Stunz LL, Hostager BS. Antigen-specific B-lymphocyte activation. Crit Rev Immunol 2003;23:149–197. [PubMed: 14584878]
4. van Kooten C, Banchereau J. CD40-CD40 ligand. J Leukoc Biol 2000;67:2–17. [PubMed: 10647992]
5. Lumsden JM, Williams JA, Hodes RJ. Differential requirements for expression of CD80/86 and CD40 on B cells for T-dependent antibody responses in vivo. J Immunol 2003;170:781–787. [PubMed: 12517941]
6. Moller G. Receptors for innate pathogen defence in insects are normal activation receptors for specific immune responses in mammals. Scand J Immunol 1999;50:341–347. [PubMed: 10520172]
7. Janssens S, Beyaert R. Role of Toll-like receptors in pathogen recognition. Clin Microbiol Rev 2003;16:637–646. [PubMed: 14557290]
8. Zuany-Amorim C, Hastewell J, Walker C. Toll-like receptors as potential therapeutic targets for multiple diseases. Nat Rev Drug Discov 2002;1:797–807. [PubMed: 12360257]
9. Bourke E, Bosisio D, Golay J, Polentarutti N, Mantovani A. The toll-like receptor repertoire of human B lymphocytes: inducible and selective expression of TLR9 and TLR10 in normal and transformed cells. Blood 2003;102:956–963. [PubMed: 12689944]
10. Bernasconi NL, Onai N, Lanzavecchia A. A role for Toll-like receptors in acquired immunity: up-regulation of TLR9 by BCR triggering in naive B cells and constitutive expression in memory B cells. Blood 2003;101:4500–4504. [PubMed: 12560217]
11. He B, Qiao X, Cerutti A. CpG DNA induces IgG class switch DNA recombination by activating human B cells through an innate pathway that requires TLR9 and cooperates with IL-10. J Immunol 2004;173:4479–4491. [PubMed: 15383579]
12. Vollmer J, Jurk M, Samulowitz U, Lipford G, Forsbach A, Wullner M, Tluk S, Hartmann H, Kritzler A, Muller C, Schetter C, Krieg AM. CpG oligodeoxynucleotides stimulate IFN-gamma-inducible protein-10 production in human B cells. J Endotoxin Res 2004;10:431–438. [PubMed: 15588427]
13. Gantner F, Hermann P, Nakashima K, Matsukawa S, Sakai K, Bacon KB. CD40-dependent and -independent activation of human tonsil B cells by CpG oligodeoxynucleotides. Eur J Immunol 2003;33:1576–1585. [PubMed: 12778475]

14. Henderson A, Calame K. Transcriptional regulation during B cell development. Annu Rev Immunol 1998;16:163–200. [PubMed: 9597128]
15. Saklatvala J, Dean J, Clark A. Control of the expression of inflammatory response genes. Biochem Soc Symp 2003:95–106. [PubMed: 14587285]
16. Peltz SW, Brewer G, Berstein P, Hart PA, Ross J. Regulation of mRNA Turnover in Eukaryotic Cells. Crit Rev Euk Gene Expr 1991;1:99–126.
17. Wilusz CJ, Wormington M, Peltz SW. The cap-to-tail guide to mRNA turnover. Nat Rev Mol Cell Biol 2001;2:237–246. [PubMed: 11283721]
18. Brewer G. Messenger RNA decay during aging and development. Ageing Res Rev 2002;1:607–625. [PubMed: 12208236]
19. Makeyev AV, Liebhaber SA. The poly(C)-binding proteins: a multiplicity of functions and a search for mechanisms. Rna 2002;8:265–278. [PubMed: 12003487]
20. Kiledjian M, Wang X, Liebhaber SA. Identification of two KH domain proteins in the α-globin mRNP stability complex. Embo J 1995;14:4357–4364. [PubMed: 7556077]
21. Leffers H, Dejgaard K, Celis JE. Characterisation of two major cellular poly(rC)-binding human proteins, each containing three K-homologous (KH) domains. Eur J Biochem 1995;230:447–453. [PubMed: 7607214]
22. Ford GS, Barnhart B, Shone S, Covey LR. Regulation of CD154 (CD40 ligand) mRNA stability during T cell activation. J Immunol 1999;162:4037–4044. [PubMed: 10201926]
23. Barnhart B, Kosinski PA, Wang Z, Ford GS, Kiledjian M, Covey LR. Identification of a complex that binds to the CD154 3′ untranslated region: implications for a role in message stability during T cell activation. J Immunol 2000;165:4478–4486. [PubMed: 11035087]
24. Kosinski PA, Laughlin J, Singh K, Covey LR. A Complex Containing Polypyrimidine Tract-Binding Protein Is Involved in Regulating the Stability of CD40 Ligand (CD154) mRNA. J Immunol 2003;170:979–988. [PubMed: 12517964]
25. Singh K, Laughlin J, Kosinski PA, Covey LR. Nucleolin is a second component of the CD154 mRNA stability complex that regulates mRNA turnover in activated T cells. J Immunol 2004;173:976–985. [PubMed: 15240685]
26. Kilger E, Kieser A, Baumann M, Hammerschmidt W. Epstein-Barr virus-mediated B-cell proliferation is dependent upon latent membrane protein 1, which simulates an activated CD40 receptor. Embo J 1998;17:1700–1709. [PubMed: 9501091]
27. Lu KT, Dryer RL, Song C, Covey LR. Maintenance of the CD40-related immunodeficient response in hyper-IgM B cells immortalized with a LMP1-regulated mini-EBV. J Leukoc Biol 2005;78:620–629. [PubMed: 15961576]
28. Tenenbaum SA, Lager PJ, Carson CC, Keene JD. Ribonomics: identifying mRNA subsets in mRNP complexes using antibodies to RNA-binding proteins and genomic arrays. Methods 2002;26:191–198. [PubMed: 12054896]
29. Livak KJ, Schmittgen TD. Analysis of relative gene expression data using real-time quantitative PCR and the 2(-Delta Delta C(T)) Method. Methods 2001;25:402–408. [PubMed: 11846609]
30. Pfaffl MW. A new mathematical model for relative quantification in real-time RT-PCR. Nucleic Acids Res 2001;29:e45. [PubMed: 11328886]
31. Zerial M, McBride H. Rab proteins as membrane organizers. Nat Rev Mol Cell Biol 2001;2:107–117. [PubMed: 11252952]
32. Hamilton BJ, Genin A, Cron RQ, Rigby WF. Delineation of a novel pathway that regulates CD154 (CD40 ligand) expression. Mol Cell Biol 2003;23:510–525. [PubMed: 12509450]
33. Fred RG, Welsh N. Increased expression of polypyrimidine tract binding protein results in higher insulin mRNA levels. Biochem Biophys Res Commun 2005;328:38–42. [PubMed: 15670747]
34. Coles LS, Bartley MA, Bert A, Hunter J, Polyak S, Diamond P, Vadas MA, Goodall GJ. A multi-protein complex containing cold shock domain (Y-box) and polypyrimidine tract binding proteins forms on the vascular endothelial growth factor mRNA. Potential role in mRNA stabilization. Eur J Biochem 2004;271:648–660. [PubMed: 14728692]
35. Pautz A, Linker K, Hubrich T, Korhonen R, Altenhofer S, Kleinert H. The polypyrimidine tract-binding protein (PTB) is involved in the post-transcriptional regulation of human inducible nitric oxide synthase expression. J Biol Chem 2006;281:32294–32302. [PubMed: 16950790]

36. Hau HH, Walsh RJ, Ogilvie RL, Williams DA, Reilly CS, Bohjanen PR. Tristetraprolin recruits functional mRNA decay complexes to ARE sequences. J Cell Biochem 2007;100:1477–1492. [PubMed: 17133347]

37. Garcia-Blanco MA, Jamison SF, Sharp PA. Identification and purification of a 62,000-dalton protein that binds specifically to the polypyrimidine tract of introns. Genes Dev 1989;3:1874–1886. [PubMed: 2533575]

38. Gil A, Sharp PA, Jamison SF, Garcia-Blanco MA. Characterization of cDNAs encoding the polypyrimidine tract-binding protein. Genes Dev 1991;5:1224–1236. [PubMed: 1906035]

39. Monie TP, Hernandez H, Robinson CV, Simpson P, Matthews S, Curry S. The polypyrimidine tract binding protein is a monomer. Rna 2005;11:1803–1808. [PubMed: 16314454]

40. Oberstrass FC, Auweter SD, Erat M, Hargous Y, Henning A, Wenter P, Reymond L, Amir-Ahmady B, Pitsch S, Black DL, Allain FH. Structure of PTB bound to RNA: specific binding and implications for splicing regulation. Science 2005;309:2054–2057. [PubMed: 16179478]

41. Xie J, Lee JA, Kress TL, Mowry KL, Black DL. Protein kinase A phosphorylation modulates transport of the polypyrimidine tract-binding protein. Proc Natl Acad Sci U S A 2003;100:8776–8781. [PubMed: 12851456]

42. Wojciechowski W, Li H, Marshall S, Dell'Agnola C, Espinoza-Delgado I. Enhanced expression of CD20 in human tumor B cells is controlled through ERK-dependent mechanisms. J Immunol 2005;174:7859–7868. [PubMed: 15944291]

43. Mizuno T, Rothstein TL. B cell receptor (BCR) cross-talk: CD40 engagement enhances BCR-induced ERK activation. J Immunol 2005;174:3369–3376. [PubMed: 15749869]

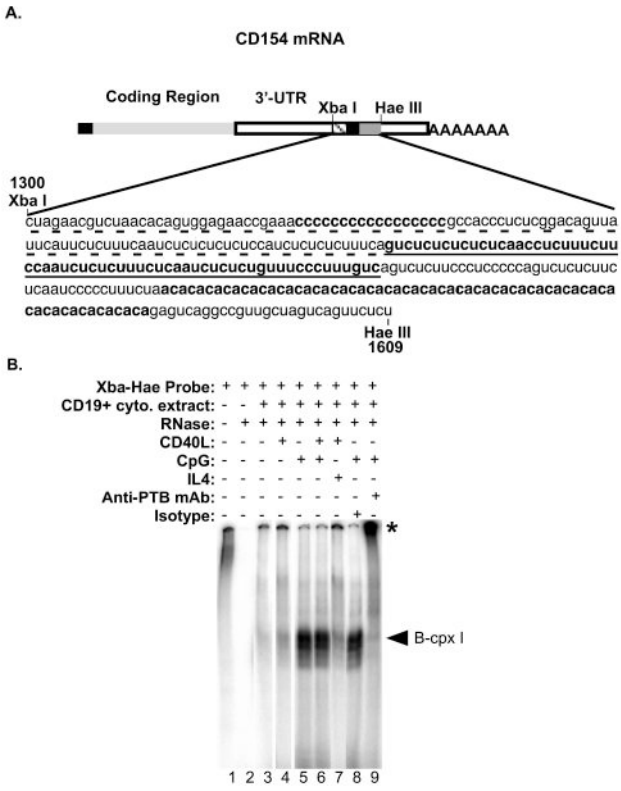

FIG. 1. An activation-induced PTB containing complex is present in CD19$^+$ cells stimulated through TLR9

(A). Schematic representation of the CD154 mRNA showing the complete sequence of the *Xba I* to *Hae III* Complex I binding region. The minimal binding site is underlined and the poly(C) tract and the CA repeats are shown in bold. (B). R-EMSA was conducted without extract (lane 2) or with 5 μg of cytoplasmic extract from CD19$^+$ cells (lanes 3-9) stimulated with CD154 alone (lane 4), CpG (lanes 5, 8 and 9), and with CD154 + IL-4 (lane 7). Control isotype (lane 8) or anti-PTB antibodies (lane 9) were added to reactions to identify PTB-containing complexes. Lane 1 is probe alone and lane 2 is probe alone with RNase. The arrow indicates the location of B-cpx I and the asterisk denotes location of super-shifted band.

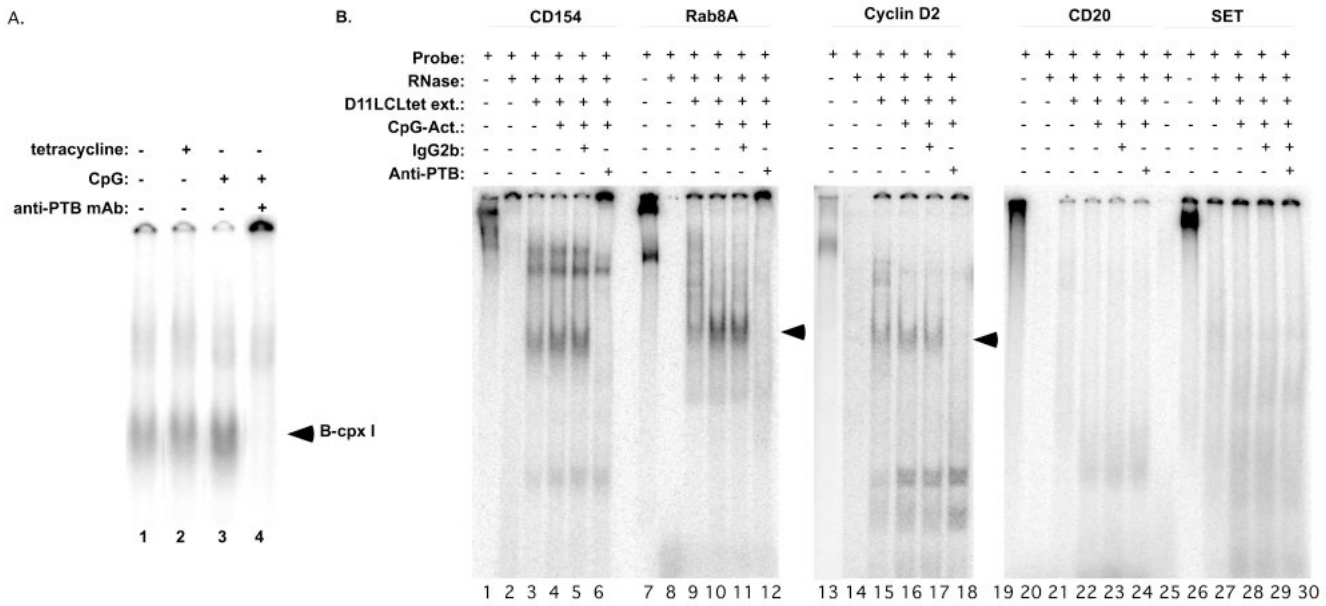

FIG. 2. B-cpx I binds to the 3′UTR of the Rab8A and Cyclin D2 transcripts

(A). To demonstrate the presence of B-cpx I in D11-LCL^{tet} cells, R-EMSA was carried out with a uniformly-labeled Xba I-Hae III CD154 probe and 5μg of cytoplasmic extracts from D11-LCL^{tet} cells grown in the absence (lane 1) or presence (lane 2) of tetracycline or without tetracycline and with 3 μM CpG for 48 h (lane 3). To confirm PTB involvement anti-PTB antibodies were added to one reaction prior to adding probe (lane 4). (B). R-EMSA was carried out with 5 μg of unstimulated (lanes 3, 9,15, 21 and 27) and CpG-stimulated (lanes 4-6, 10-12,16-18, 22-24 and 28-30) D11-LCL^{tet} cytoplasmic extract and uniformly labeled 3′UTR probes from CD154 (lanes 1-6), Rab8A (lanes 7-12), cyclin D2 (lanes 13-18), CD20 (lanes 19-24) and SET (lanes 25-30). Anti-PTB (lanes 6, 12, 18, 24 and 30) and control (lanes 5, 11, 17, 23 and 29) antibodies were added to reactions to demonstrate the presence of PTB in B-cpx I.

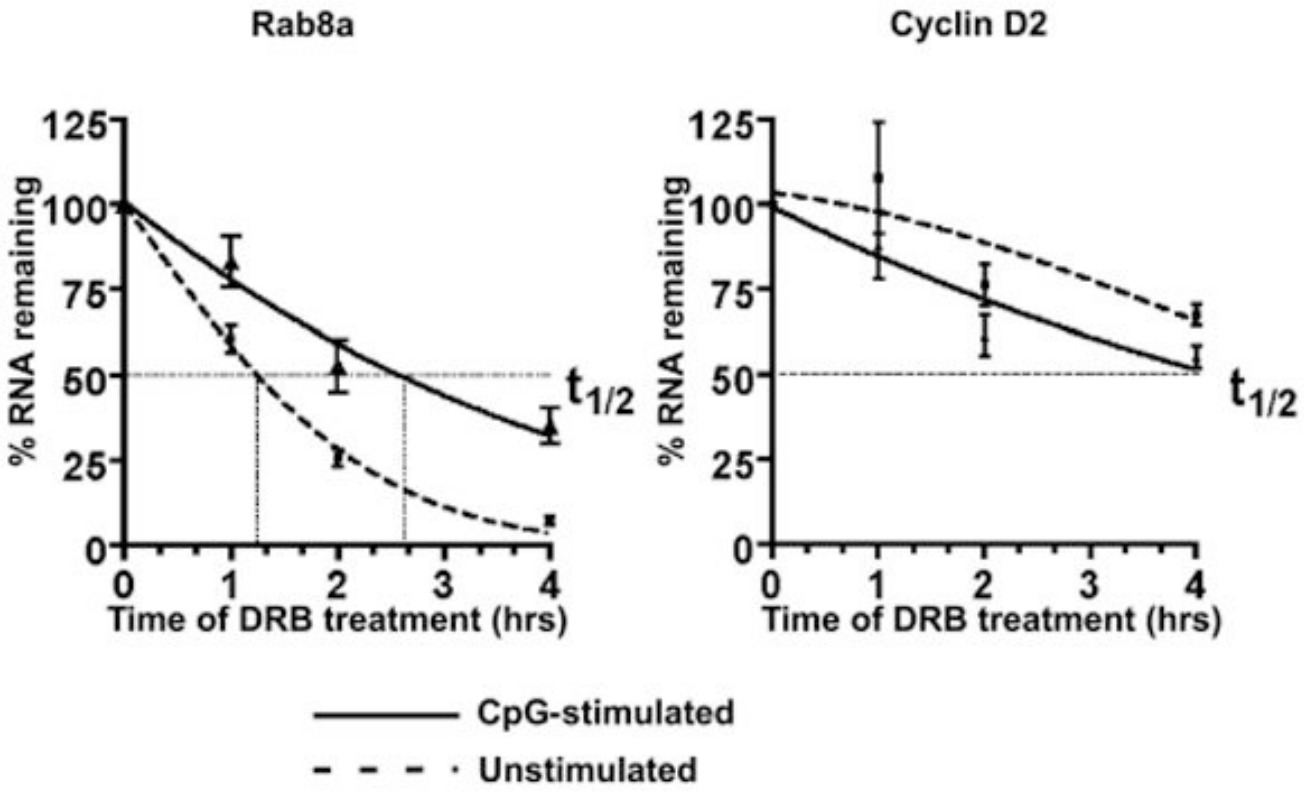

FIG. 3. The Rab8A but not the Cyclin D2 transcript is stabilized in response to CpG-mediated B cell activation

Aliquots of unstimulated (dashed line) and 48 h CpG-stimulated (solid line) $CD19^{+}/IgG^{-}$ cells were incubated with DRB for 1 h, 2 h and 4 h. RNA was isolated from the different fractions, reverse transcribed and amplified with primers specific for the Rab8A (left panel) and Cyclin D2 (right panel) transcripts. The dashed, vertical lines denote the $t_{1/2}$ of the transcripts normalized to 28S rRNA. Each time point represents the average and SEM of three independent experiments. Curve-fitting was performed by nonlinear regression.

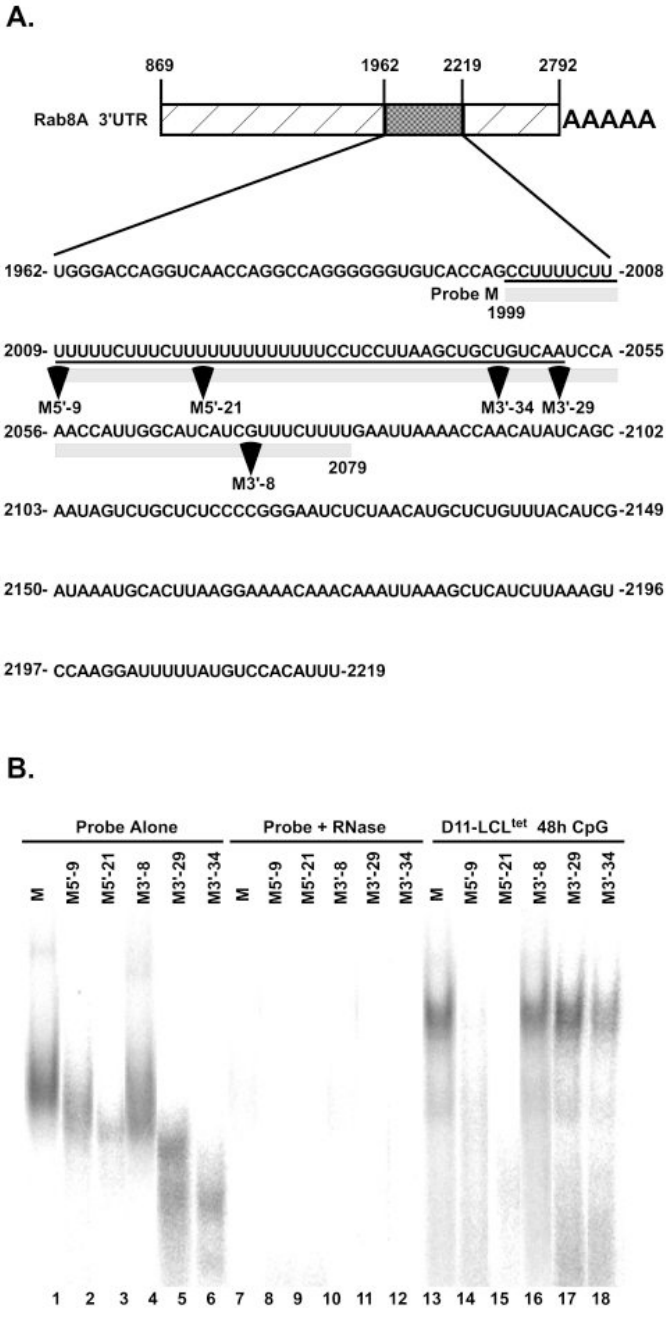

FIG. 4. A 52 nt sequence is identified as a B-cpx I binding site in the Rab8A transcript

(A). Shown is the representation of the Rab8A 3′UTR. The gray stippled box bound by nt 1962 and 2219 represents the region assayed for B-cpx I binding in R-EMSAs. Underlined is the CU-rich stretch that shows specific binding to PTB. Rab8A probes spanning nt 1999 to 2079 are indicated by the box under the RNA sequence shown and are used in R-EMSA reactions shown in B. (B). R-EMSA was carried out with Rab8A probes as indicated (lanes 13-18). Lanes 1-6 show R-EMSA reactions with probe alone and no extract and lanes 7-12 are reactions containing probe with RNase but without extract.

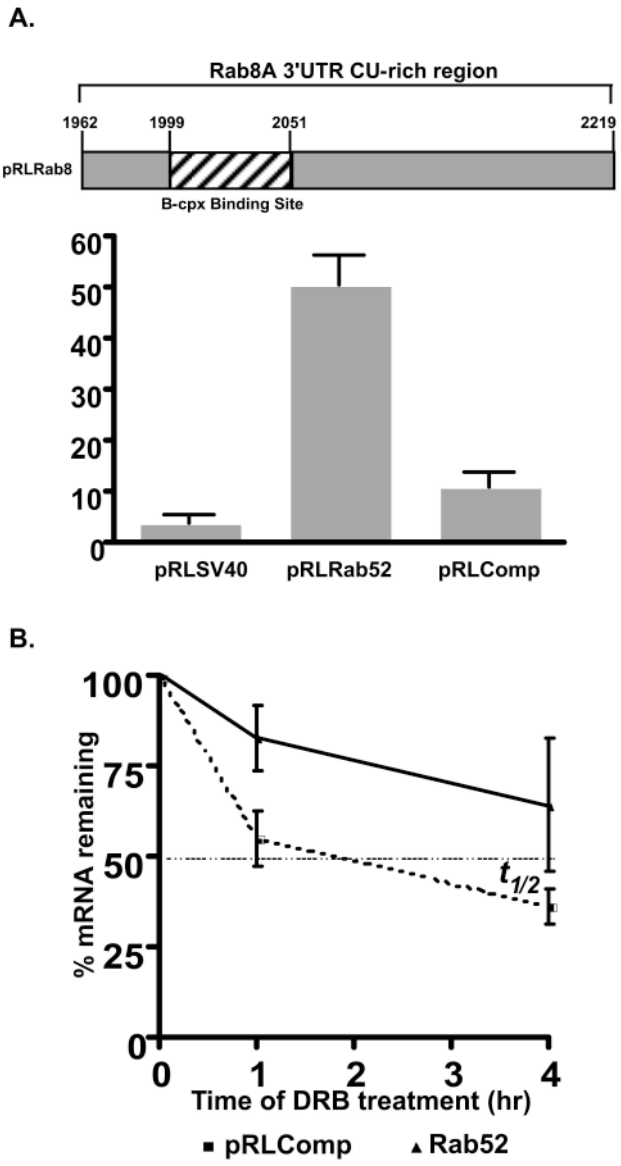

FIG. 5. The Rab8A minimal binding region increases the expression of a heterologous transcript

(A). Top schematic shows the 52 nt minimal binding region from the Rab8A 3′UTR. This region was cloned into the 3′UTR of the pRLSV40 vector either in the correct (pRLRab52) or reverse (pRLComp) orientations, transiently transfected into CpG-stimulated D11-LCL^{tet} cells with a constant amount of pGL2 (vector expressing Firefly luciferase) and Renilla and Firefly luciferase activity measured from total cell extracts 48 h later. The results represent the average of three independent experiments. (B). D11-LCL^{tet} cells were transiently transfected using Amaxa technology with the pRLRab52 and pRLComp constructs followed by stimulation with CpG. After 24 hr, transcription was inhibited by the addition of 50μg/ml DRB and 3×10^6 cells were collected for each time point over a 4 h time course. Plotted is the percent RNA remaining from each time point. Triplicate samples of cDNA from each time point were analyzed by qPCR. Results are the average of two independent experiments.

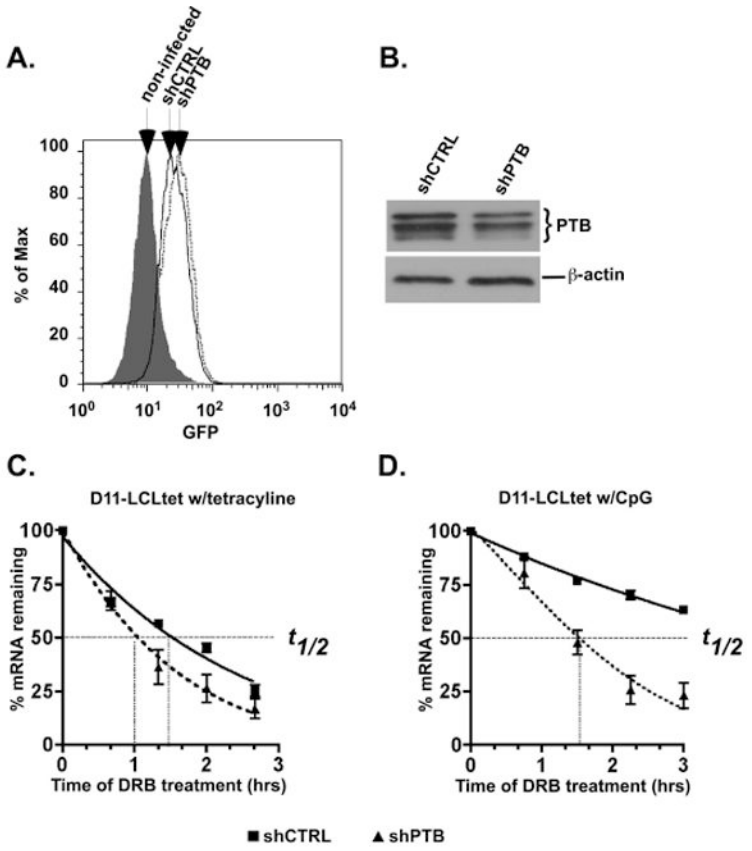

FIG. 6. Down-regulating PTB decreases the stability of the Rab8A transcript in CpG-activated D11-LCL^{tet} cells

(A) D11-LCL^{tet} cells were infected with virus expressing either the pLVTHM-U6-shPTB or the pLVTHM-U6-shCTRL vector and four days later analyzed by FACS for expression of eGFP. (B). Western blot analysis of PTB expression in cytoplasmic extracts from D11-LCL^{tet} cells expressing either shPTB or shCTRL four days after infection. β-actin is used as a loading control. (C and D). The stability of the endogenous Rab8A transcript was analyzed using DRB inhibition of transcript elongation. D11-LCL^{tet} cells were infected with either shPTB or shCTRL and either left non-activated (C) or activated with CpG activation for 24 h (D). Four days later, DRB was added to the cultures and RNA isolated from cells removed over a 3 h time course.

Table I

Transcripts Enriched in 3 Separate Microarray Screenings[a]

		CD19+ B Cells		CD19+ B Cells		CD19+/IgG- B Cells	
Accession Number	**Gene Name/ Description**	**Array 1 FC**	**P-value Array 1**	**Array 2 FC**	**P-value Array 2**	**Array 3 FC**	**P-value Array 3**
NM_020151.1	GTT1 (phosphatidylcholine transfer protein-like)	4	0.00013	3.0	0.00002	8	0.00004
NM_003011.1	SET gene, translocation myeloid leukemia-associated	4.9	0.000865	3.5	0.00002	7.5	0.00004
NM_005566.1	lactate dehydrogenase A	18.4	0.000078	4.0	0.00002	7.0	0.00002
NM_005722.1	ARP2 actin-related protein 2	6.1	0.000167	2.5	0.00004	5.3	0.000101
NM_004965.1	high-mobility group (nonhistone chromosomal) protein 14 (HMG14)	8.6	0.000438	2.3	0.000307	4.0	0.00004
NM_001759.1	cyclin D2 (CCND2)	10.6	0.00002	3.5	0.000273	8.0	0.00002
NM_021038.1	muscleblind (Drosophila)-like (MBNL)	3.5	0.000774	2.0	0.000774	6.5	0.00002
NM_005839.1	SerArg-related nuclear matrix protein (SRM160)	19.7	0.001651	2.6	0.00002	3.5	0.00002
BE966236	ribonucleotide reductase M2 polypeptide	11.3	0.000492	5.7	0.00002	5.3	0.00002
NM_004642.1	deleted in oral cancer (mouse, homolog) 1 (DOC1), CDK2-associated protein 1 (CDK2AP1)	6.1	0.00003	3.7	0.00002	8.6	0.00003
NM_015361.1	Homo sapiens R3H domain containing 1 (R3HDM1)	9.8	0.000552	2.5	0.00002	4.9	0.000052
NM_007057.1	ZW10 interactor (ZWINT)	137.2	0.000618	5.7	0.000078	3.7	0.000865
NM_016817.1	2-5oligoadenylate synthetase 2 (OAS2), transcript variant 1	4.9	0.000167	2.0	0.000027	4.6	0.000492
NM_004728.1	DEADH (Asp-Glu-Ala-AspHis) box polypeptide 21 (DDX21)	4.9	0.001486	2.1	0.00002	3.2	0.001832
BC003689.1	high-mobility group (nonhistone chromosomal) protein 17	5.7	0.001077	2.0	0.000114	2.8	0.00002
AF279893.1	PNAS-139 mRNA, Human acute promyelocytic leukemia cell line NB4's apoptosis/differentiation related genes	16.0	0.000046	2.0	0.000241	5.3	0.000389
BC000903.1	high-mobility group (nonhistone chromosomal) protein 2	9.8	0.001832	2.8	0.00002	8.0	0.00013
BC002977.1	mel transforming oncogene (derived from cell line NK14)- RAB8 homolog	22.6	0.000346	3.5	0.00002	3.0	0.00002
BC005299.1	cytochrome c	4.3	0.000023	2.6	0.00002	3.0	0.000273

		CD19+ B Cells		CD19+ B Cells		CD19+/IgG- B Cells	
Accession Number	**Gene Name/ Description**	**Array 1 FC**	**P-value Array 1**	**Array 2 FC**	**P-value Array 2**	**Array 3 FC**	**P-value Array 3**
L07555.1	early activation antigen CD69	4.9	0.000273	3.0	0.00002	7.5	0.000046
D14826.1	hCREM (cyclic AMP-responsive element modulator) type 2 protein	6.1	0.000346	4.9	0.00002	2.5	0.000552
BG538627	Homo sapiens mRNA; cDNA DKFZp586I2022 (from clone DKFZp586I2022)	7.5	0.00002	2.0	0.000068	2.8	0.000618
AI984005	exportin, tRNA (nuclear export receptor for tRNAs)	7.0	0.001077	3.5	0.00002	16.0	0.000114
X76302.1	putative nucleic acid binding protein	11.3	0.001336	2.1	0.000023	4.9	0.00002
AF091078.1	Homo sapiens clone 559 unknown mRNA, complete sequence.	2.3	0.001336	3.2	0.00002	7.0	0.000101
X12530.1	B lymphocyte antigen CD20 (B1, Bp35)	24.3	0.001486	3.0	0.00003	4.0	0.000114
NM_016359.1	nucleolar and spindle associated protein 1 (NUSAP1)	48.5	0.00002	4.6	0.00002	7.5	0.000023
AW612574	hypothetical protein MGC5350	2.5	0.000865	2.6	0.00002	27.9	0.00004
AB037814.1	Homo sapiens mRNA for KIAA1393 protein, partial cds.	5.7	0.000552	2.0	0.00002	3.0	0.00003
U10485	Human lymphoid-restricted membrane protein (Jaw1)	4.0	0.000191	2.6	0	9.8	0.001876
NM_016294.1	serinethreonine protein phosphatase catalytic subunit (LOC51723), mRNA	7.0	0.001486	3.7	0.00002	5.3	0.00002

[a]Thirty-one transcripts are commonly enriched by anti-PTB from CpG-stimulated B cells in 3 microarray screenings. Transcripts were selected based on a 2-fold or greater enrichment by immunoprecipitation with anti-PTB antibodies in the CpG stimulated versus resting B cells. P-values shown are change of P-values calculated in a comparison analysis of each set of arrays using the resting B cells as a baseline.

Table II

Confirmed PTB-interacting transcripts from CpG-activated B cells[a]

	1	2	3
cyclin D2 (CCND2)	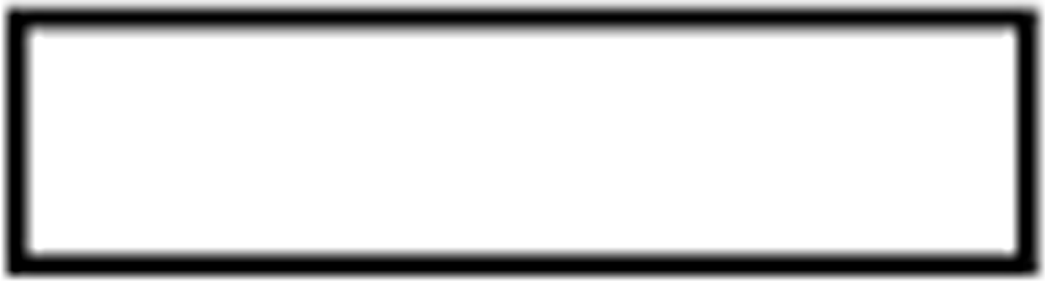		
muscleblind (drosophila)-like (MBNL)	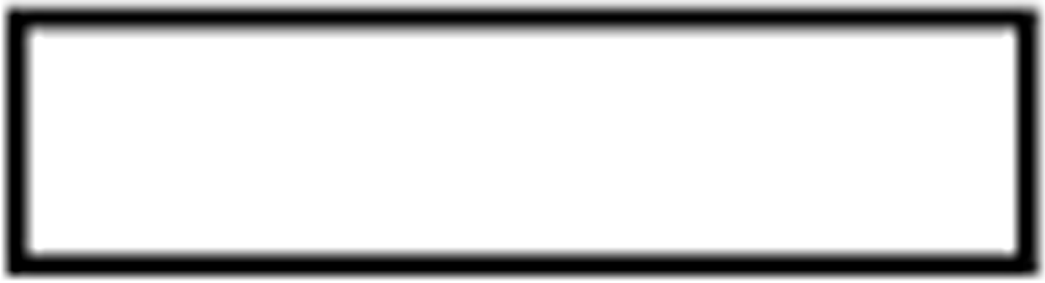		
serinethreonine protein phosphatase catalytic subunit (LOC51723)	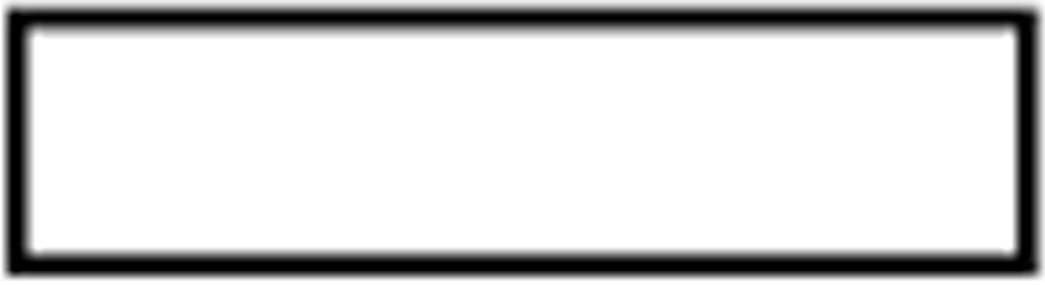		
mel transforming oncogene – RAB8 homolog	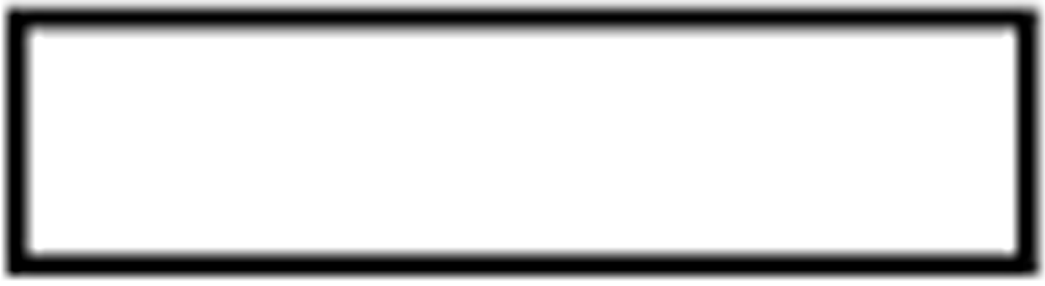		

	1	2	3
B lymphocyte antigen (CD20 (B1, Bp35)	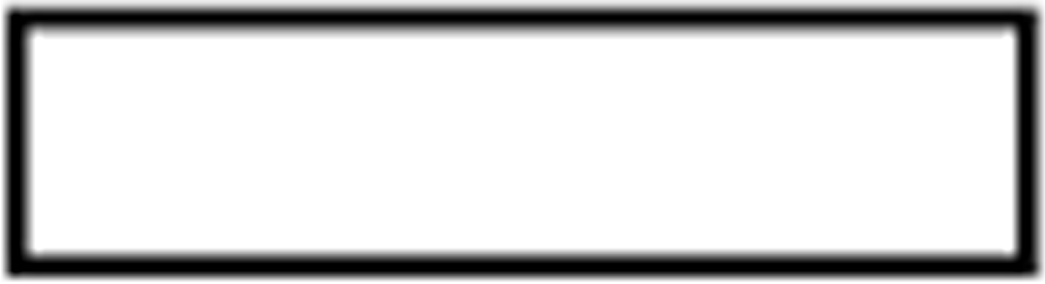		
SET gene, translocation myeloid leukemia-associated	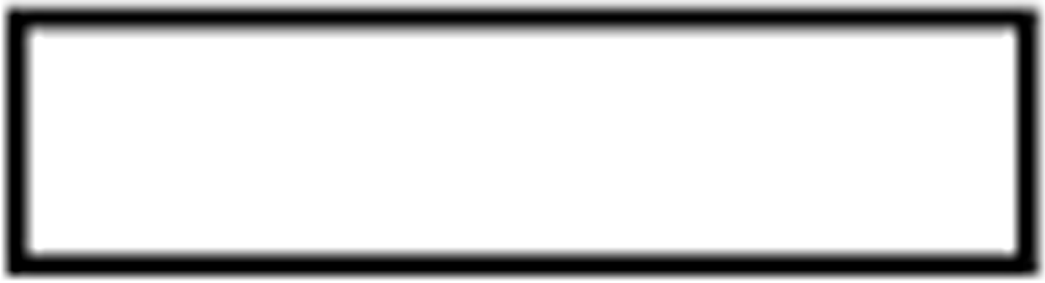		
nucleolar and spindle associated protein 1 (NUSAP1)	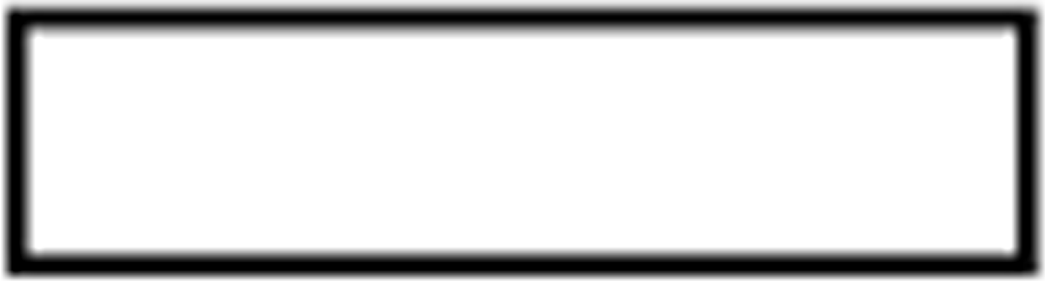		
high-mobility group (nonhistone chromosomal) protein 17	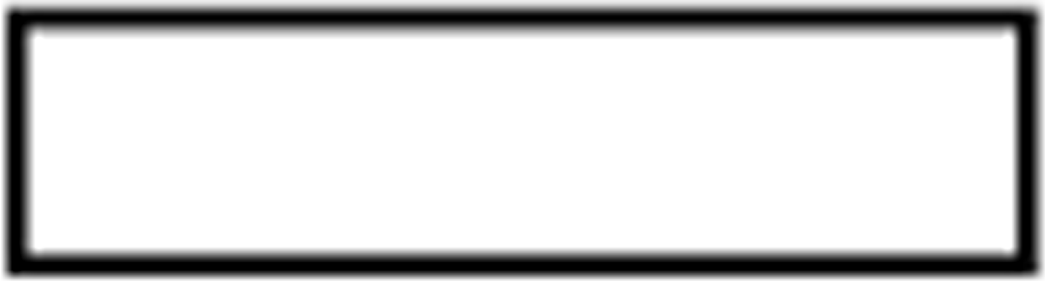		
SerArg-related nuclear matrix protein (SRM160)	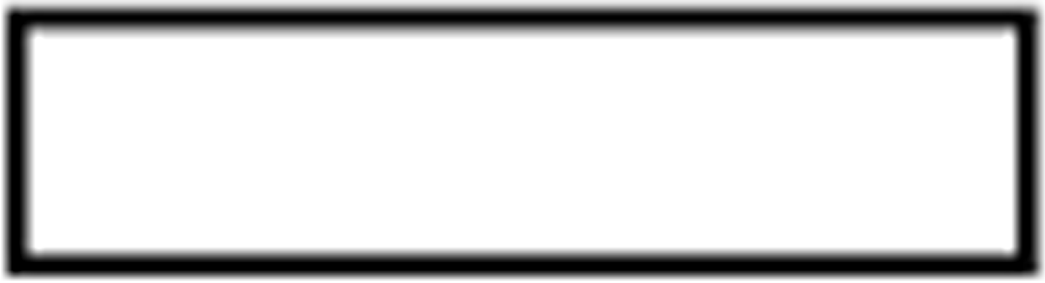		

	1	2	3
homo sapiens R3H domain containing 1 (R3HDM1)	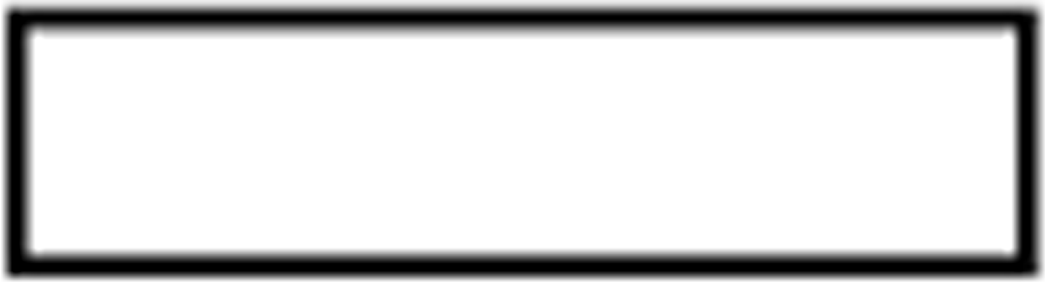		
ZW10 interactor (ZWINT)	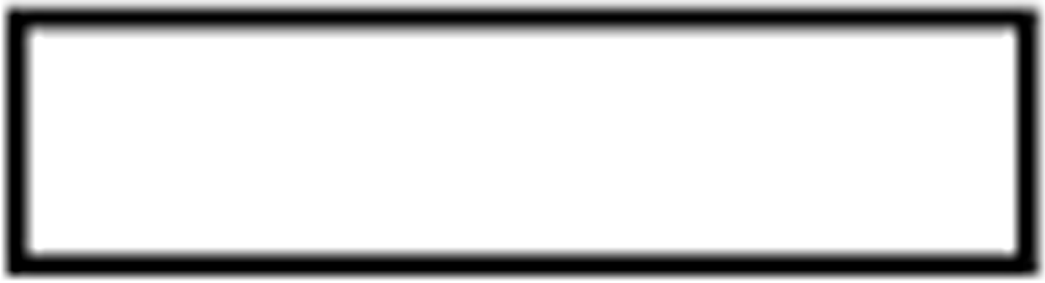		
2-5 oligoadenylate synthetase 2 (OA S2), transcript variant 1	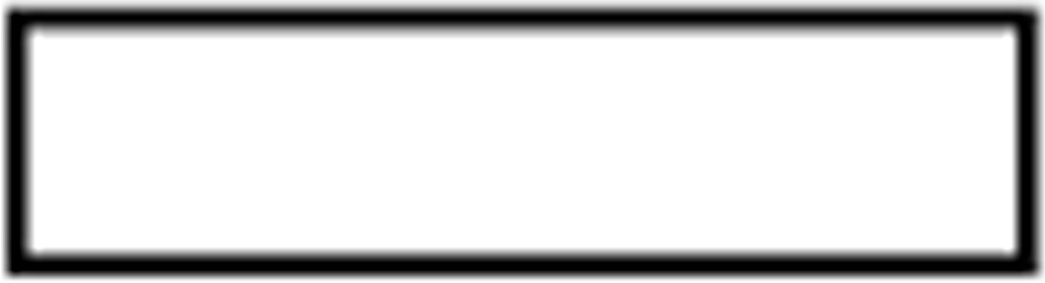		
early activation antigen CD69	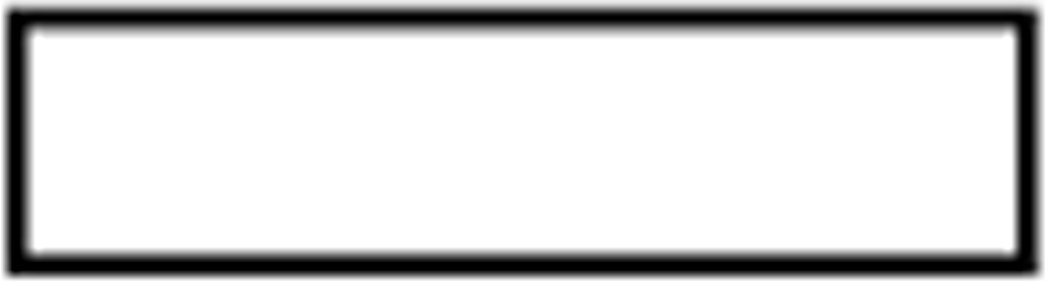		
high-mobility group protein 14 (HMG14)	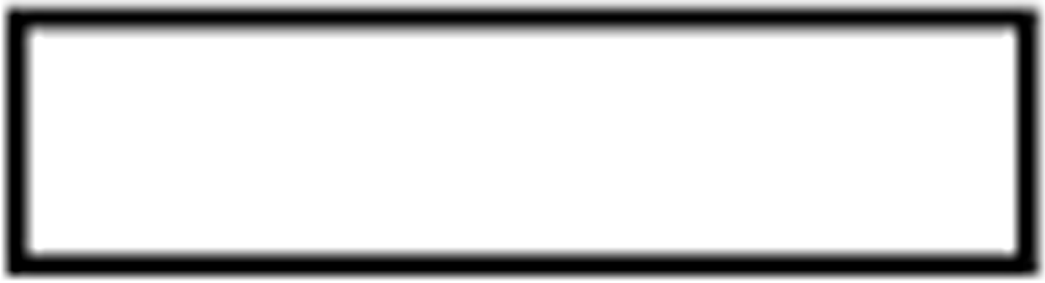		

	1	2	3
GTT1 (phosphatidylcholine transfer protein-like)	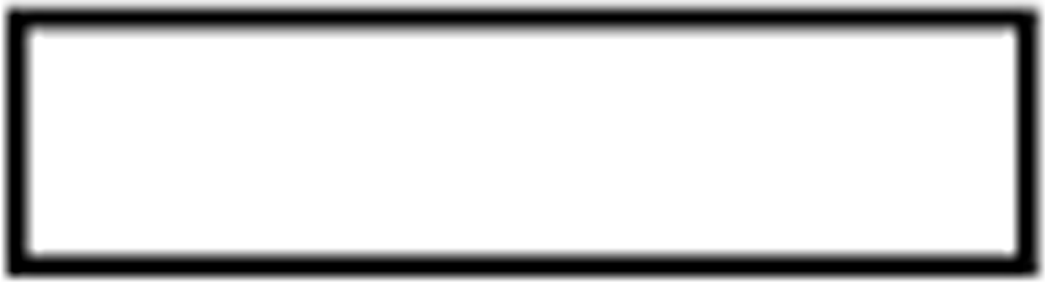		
lactate dehydrogenase A	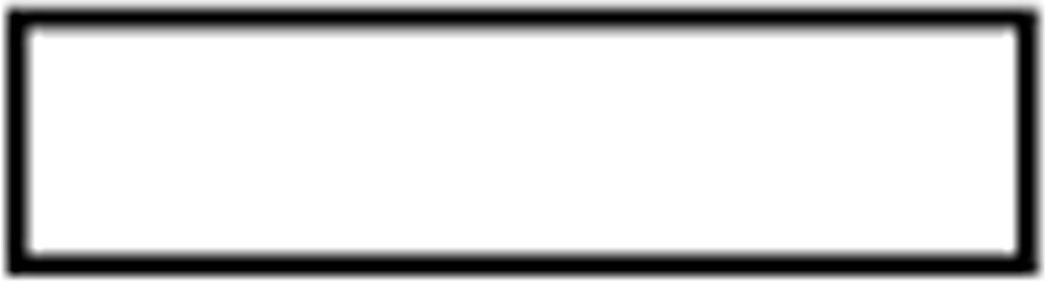		
ARP2 actin-related protein 2	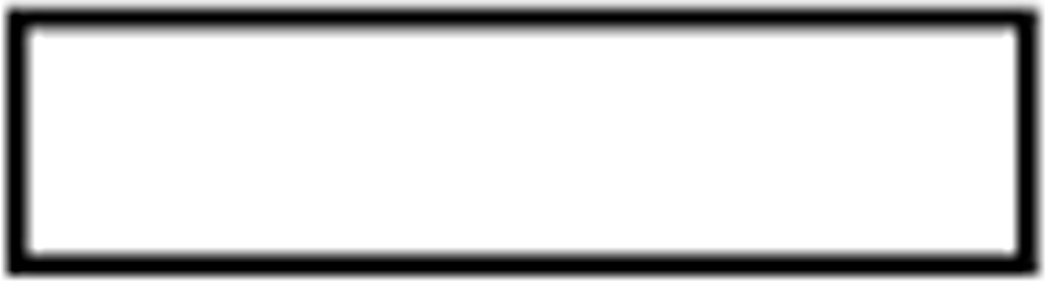		
hCREM (cyclic AMP-responsive element modulator) type 2 protein	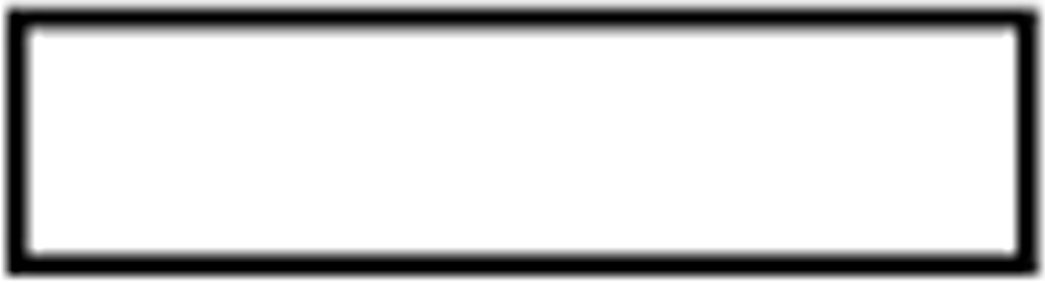		
deleted in oral cancer (mouse, homology) 1 (DOC1)	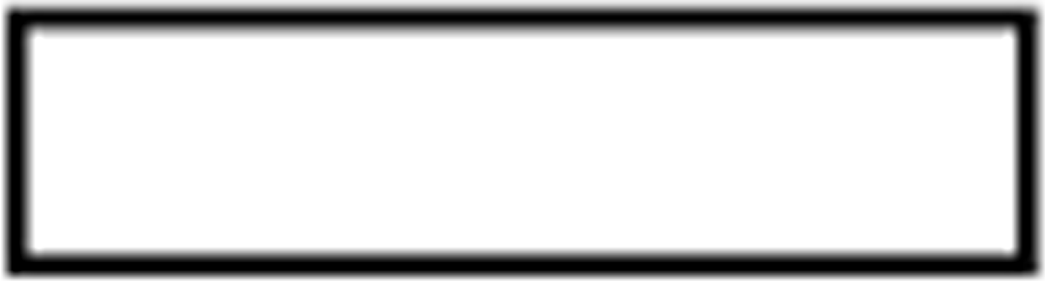		

	1	2	3
DEADH (Asp-Glu-Ala-AspHis) box polypeptide 21 (DDX21)	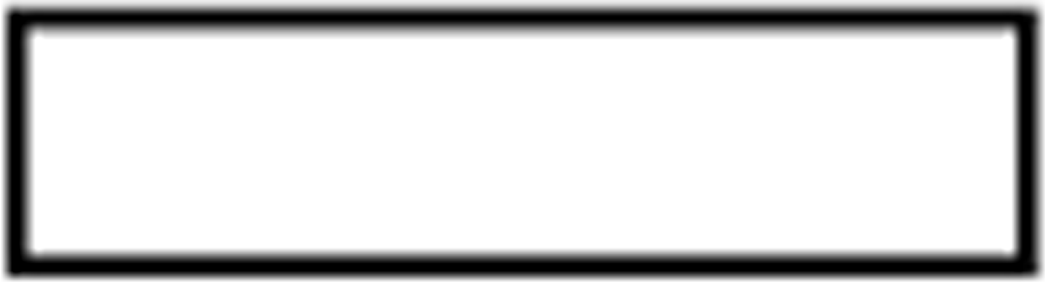		
PNAS-139 mRNA	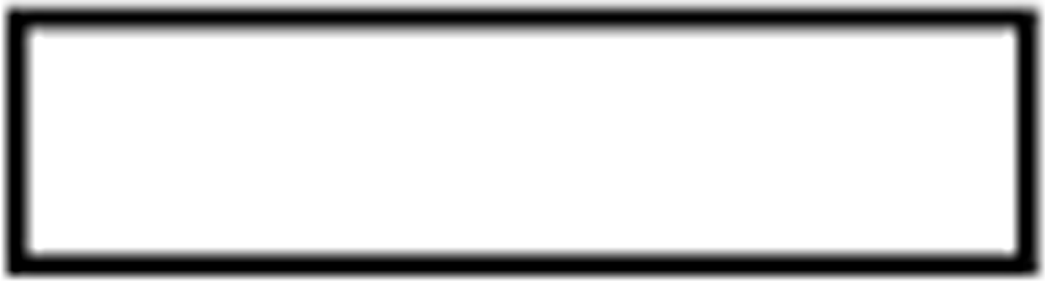		
high-mobility group (nonhistone chromosomal) protein 2	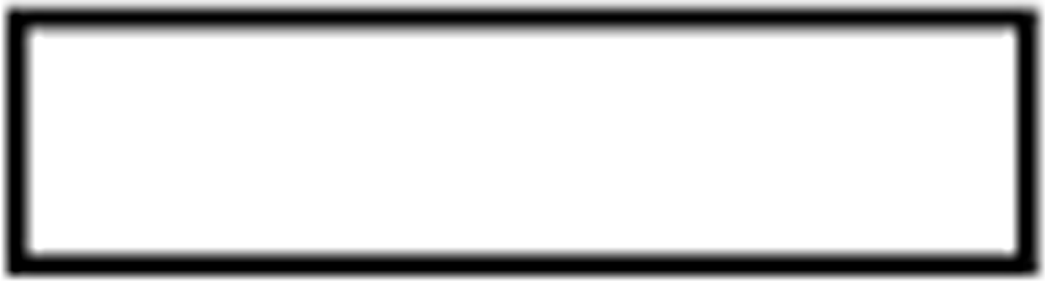		
cytochrome c	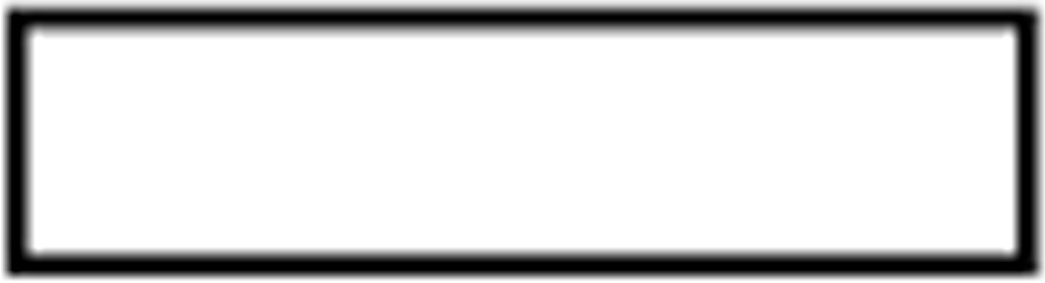		
putative nucleic acid binding protein	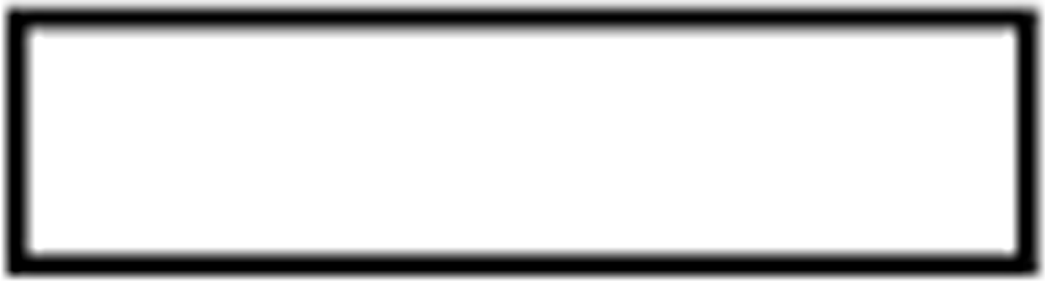		

	1	2	3
human lymphoid-restricted membrane protein (Jaw1)	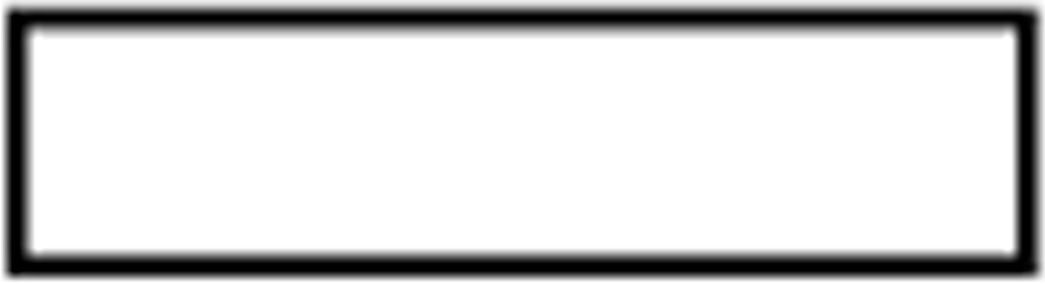		
GAPDH	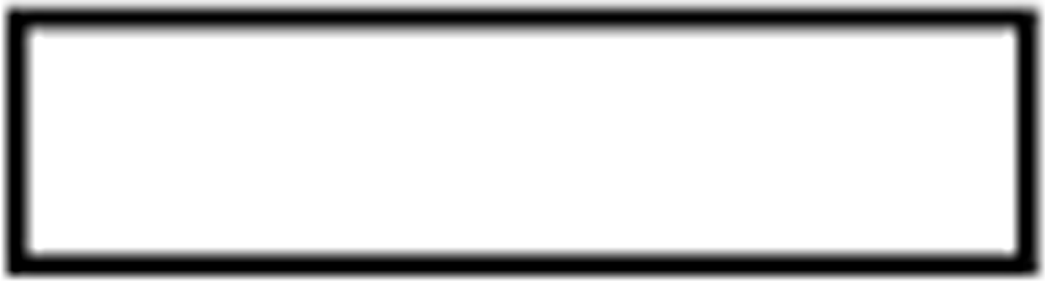		
β-actin	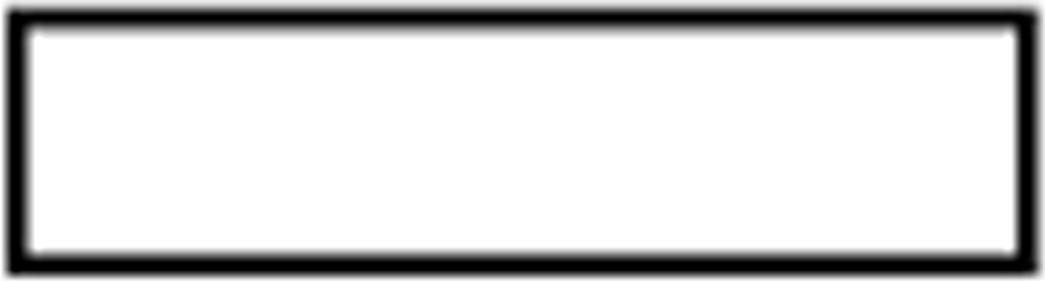		

[a] $CD19^+$ B cells were stimulated for 48 h with 3 mM CpG and cytoplasmic extracts immunoprecipitated with either anti-PTB (lane 1) or isotype control (lane 2) antibodies and the RNA isolated, reverse transcribed and amplified with primers specific for the indicated genes. Cytoplasmic RNA isolated from CpG-activated B cells was used as a control in all reactions (lane 3).